Neutron diffraction study of mechanically alloyed and *in situ* annealed $Al_{75}Mo_{25}$ powders

S. Enzo
Istituto Nazionale di Fisica della Materia INFM e Dipartimento di Chimica dell'Università di Sassari, via Vienna 2, 07100 Sassari, Italy

R. Frattini[a)]
INFM e Dipartimento di Chimica Fisica dell'Università di Venezia, Dorsoduro 2137, 30123 Venezia, Italy

P. Canton
Dipartimento di Chimica Fisica dell'Università di Venezia, Italy

M. Monagheddu and F. Delogu
Istituto Nazionale di Fisica della Materia (INFM) e Dipartimento di Chimica dell'Università di Sassari, via Vienna 2, 07100 Sassari, Italy

(Received 20 October 1999; accepted for publication 14 December 1999)

The mechanical treatment of a $Al_{75}Mo_{25}$ mixture of pure elemental powders in a high-energy mixer mill induces partial solid state reactivity and solid solution formation. This is suggested by a quantitative phase evaluation and by the changes of Al lattice parameter carried out with Rietveld analysis of diffraction patterns collected after extended time of processing (4, 8, 16, 32, 57, and 78 h). The small angle neutron scattering experiments showed that diffusion processes are the rate-controlling step for these solid state reactions. The formation of metastable phases is confirmed by *in situ* neutron diffraction annealing experiments on selected as-milled powders. In the specimen mechanically alloyed for 4 h, $Al_{12}Mo$ phase is formed at 590 °C (below the aluminum melting point). Soon after this temperature, the remaining Al is consumed to form the Al_8Mo_3 phase. In the alloy mechanically treated for 32 h, the $Al_{12}Mo$ phase appears after annealing at 430 °C, while the Al_8Mo_3 phase is found at 493 °C. After the disappearance of $Al_{12}Mo$ phase (500 °C), the solid state reaction proceeds to form a new tetragonal Al_3Mo phase, not reported in the equilibrium phase diagram. In the specimen mechanically treated for 57 h, the total formation of Al_8Mo_3 is recorded at 430 °C. Conversely, in the powder ball milled for 78 h, the Al_8Mo_3 phase appears at 390 °C and coexists with tetragonal Al_3Mo. © *2000 American Institute of Physics.* [S0021-8979(00)06406-9]

I. INTRODUCTION

In the last decade, the synthesis of aluminum-based nanocrystalline materials has been carried out especially by mechanical alloying (MA) or, alternatively, by mechanical milling[1,2] because of the relatively high productivity of the method. As a matter of fact, such a treatment of materials has been found to improve to an appreciable level the physical, mechanical, structural, and electrocatalysis properties.[3] A large number of studies so far reported in the literature have dealt with Al–Ni, Al–Ti, and Al–Fe alloys.[4–6] The Al-rich side compositions of binary alloys deserve importance due to the low density accompanied with good corrosion resistance.

Previous diffraction studies on Al–Fe alloys[7–10] have pointed out difficulties for a full microstructure characterization during the course of the processing. This is essentially due to the lattice parameter mismatch between fcc Al and bcc Fe, such as to make all the bcc peaks coincident to the fcc peaks with indices all even (e.g., 200, 220, 222, etc.).[11] To avoid this drawback, we turned to the Al–Mo system, which is supposed not only to avoid significant peak overlapping of two parental phases, but also to behave isotropically versus the lattice damage brought about by the mechanical treatment.[12] Only one group has so far reported an investigation of the Al–Mo system.[13–15] It was pointed out the possibility of creating very fine composite powders and that the amount of molybdenum entrapped in supersaturated solution increased with the molybdenum content in the powders. However, the formation of solid solution and the appearance of amorphous phase remained an open question.[15] We present our results in the expectation to bring more details to the mechanisms of solid state reactivity of Al-based alloys. Therefore, the structural behavior of $Al_{75}Mo_{25}$ alloys, produced by MA of pure elemental powders was studied as a function of treatment time by means of x-ray diffraction and as a function of annealing temperature by means of the constant wavelength neutron diffraction instrument D20 of Grenoble (France), equipped with a furnace facility for *in situ* heating.

II. EXPERIMENTAL PROCEDURE

Samples in the atomic composition $Al_{75}Mo_{25}$ were produced after mixing aluminum and molybdenum powders of 99.99 wt. % purity. The milling was performed for 4, 8, 16, 32, 57, and 78 h in a hardened steel vial using a Spex mixer/mill model 8000, under an inert atmosphere of argon. Etha-

a)Electronic mail: frattini@unive.it

 © 2000 American Institute of Physics

Downloaded 18 Nov 2008 to 192.167.65.40. Redistribution subject to AIP license or copyright; see http://jap.aip.org/jap/copyright.jsp

nol as a lubricant agent was added in concentration of 0.05 ml/g of powder to avoid aluminum sticking to the milling media and to slow down the process for complete evaluation of fine details.

Differential scanning calorimetry (DSC) experiments were carried out with a Perkin–Elmer DSC7 instrument with a graphite crucible, under argon flow at heating rate of 20 K/m.

X-ray diffraction (XRD) patterns were collected with a Bragg–Brentano powder diffractometer using Cu $K\alpha$ radiation ($\lambda = 1.54178$ Å) and a graphite monochromator in the diffracted beam.

Neutron diffraction measurements were performed at the instrument D20 of ILL Laboratory in Grenoble (France). The wavelength employed was 1.2946 Å as determined after calibration. The heating ramp velocity varied from 50 to 100 °C/h and an entire pattern was collected each 5 min approximately.

Diffraction data were analyzed with the Rietveld method,[16] using the FULLPROF[17] and the RIETQUAN codes.[18] While the first program is used according to the methodology reported in our previous publications,[11] the latter, in a fully automated version, is particularly suited for a quantitative evaluation of phases present in x-ray diffraction patterns. Contrary to previous works on this system,[14,15] the parameters of physical meaning such as lattice constant, phase abundance, average crystallite size, and microstrain are worked out from the full pattern analysis and not by comparative investigation of the peak broadening after analysis for each peak.

The neutron small angle scattering (SAS) experiments were conducted on the low-Q (LOQ) instrument at the ISIS neutron source, Rutherford Appleton Laboratory (RAL), Chilton (UK). The samples were contained in Hellma cells and the SAS data were analyzed using the COLETTE package on the LOQ instrument.

III. RESULTS AND DISCUSSION

A. As-milled specimens

Figure 1 shows the neutron small angle curves for milled alloys. The departure from the -4 slope value of parents is typical of dissipative processes in reactive systems and can be evaluated quantitatively with an index of ''fractal'' dimension. As it can be seen for all the processed alloys, the slope value -2.7 gives a characteristic fractal dimension of 3.3, similar to our previous work in other binary metal systems.[19,20]

Figure 2 shows the XRD diffraction patterns of specimens MA for the times quoted. For a comprehensive view of structural features, we have reported the intensity data in a logarithmic scale to evaluate also high *hkl* peaks at high-Q scattering vector, which otherwise would had not appreciated using a linear scale. In the powder pattern of parents, the $K\alpha_1 - \alpha_2$ splitting is well evident in the high-Q peaks but is evaluated also after a close inspection of data of low-order peaks at low-Q, confirming the setup for high resolution of our instruments. The correspondent neutron measurements, reported in Ref. 21, show, as expected, a similar behavior.

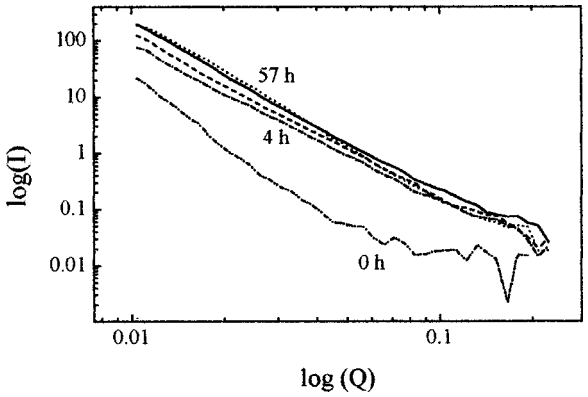

FIG. 1. Neutron small angle curves for $Al_{75}Mo_{25}$. The feature of 0 h MA powder (dashed-double-dotted line) present a slope value equal to -4. The features referring to 4 h MA (dashed-dotted line), 8 h MA (dashed line), 32 h MA (full line), and 57 h MA (dotted line) shows a similar behavior, the slope values are -2.7.

However, the low instrumental resolution and the presence of iron peaks due to furnace misalignment, made it difficult for the precise evaluation of lattice parameters for 0 and 32 h MA specimens respectively, so these data are associated to a larger bar error and should be taken with more caution. In the sequence of the patterns, it can be seen that a large peak broadening of both fcc and bcc phases is induced by the mechanical treatment already after 4 h. Analysis of the peak shape parameters achieved with the Rietveld strategy of best fitting (full lines) suggests that the broadening can be ascribed to simultaneous lattice disorder and crystallite size

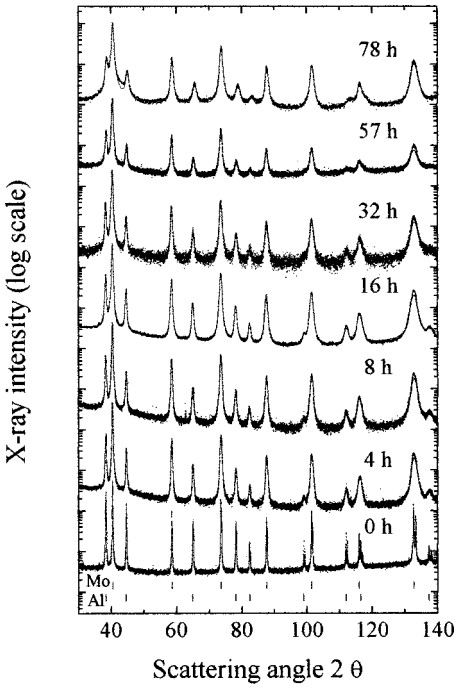

FIG. 2. XRD patterns (data points) and Rietveld fit (full lines) of $Al_{75}Mo_{25}$ powders mechanically treated for the times indicated. A significant decrease of the fcc spectrum can be observed after 4 h of MA. Small changes in the peak positions suggest that the lattice parameter variations subsequent to milling are very small. The considerable line broadening is ascribable to simultaneous lattice strain and crystallite size reduction.

Downloaded 18 Nov 2008 to 192.167.65.40. Redistribution subject to AIP license or copyright; see http://jap.aip.org/jap/copyright.jsp

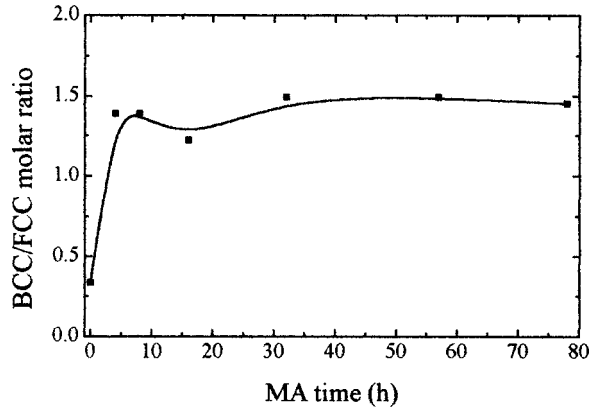

FIG. 3. Molar ratio of bcc/fcc phases as a function of processing time. These figures were obtained by assuming the electron density in the lattice determined by just one atomic species, which is true only for the parent specimen.

effects. This can also be thoroughly evaluated by the fact that, for the bcc phase in Fig. 2, the peak broadening ratio $\beta(4\,\mathrm{h})_{110}/\beta(0\,\mathrm{h})_{110}$ is certainly much smaller than $\beta(4\,\mathrm{h})_{321}/\beta(0\,\mathrm{h})_{321}$. Thus, assuming that the broadening of the 0 h specimen represents the instrument function, this observation means that the peak broadening is *hkl* or *Q* dependent, which in turn implies the presence of lattice strain. In Fig. 2, we can also observe decrease of the fcc phase, so it

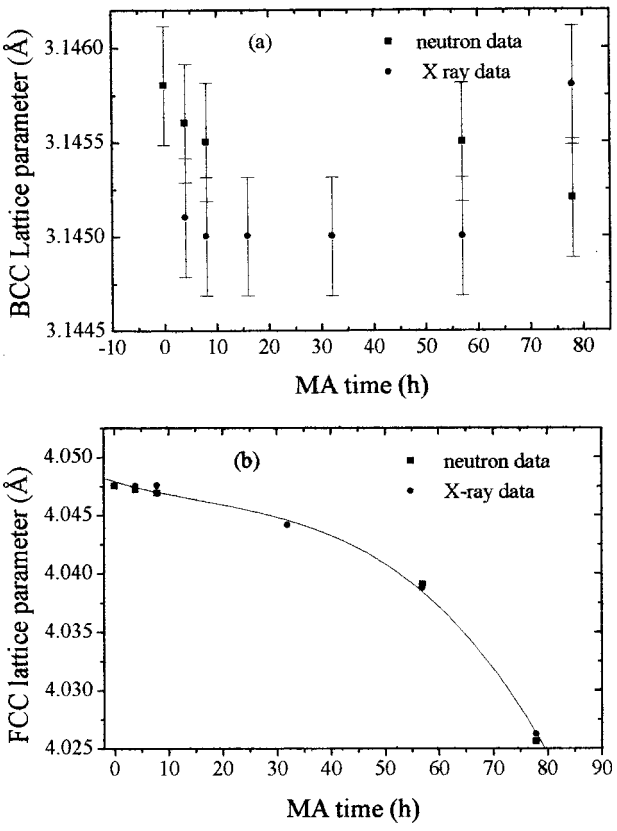

FIG. 4. Lattice parameter behavior of (a) bcc and (b) fcc phases during the MA process. Full squares refers to data obtained from neutron diffraction measurements, full circles refers to data obtained from x-ray patterns. Note that the bcc phase does not show significant changes within the experimental uncertainty. (b), the points are connected by a spline curve.

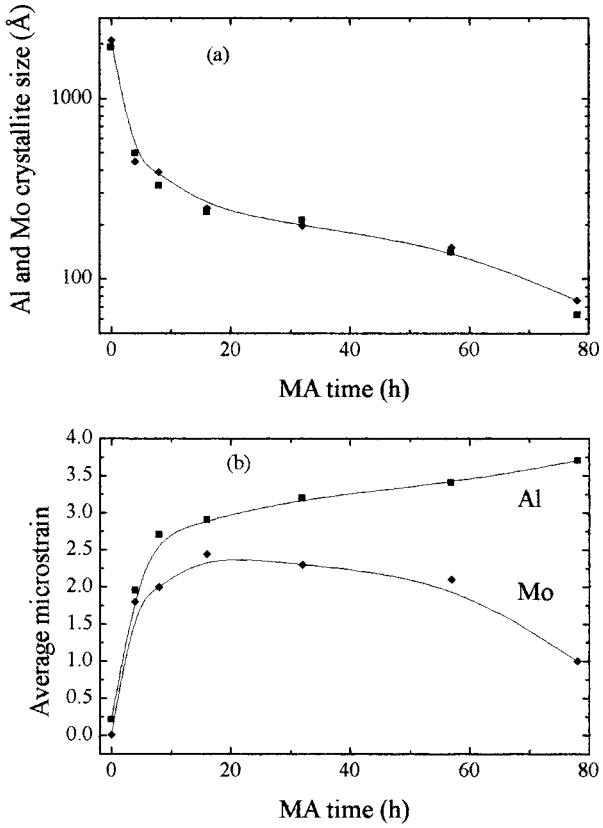

FIG. 5. (a) Average crystallite size and (b) mean squared lattice strain as a function of milling time. Full squares refers to the fcc phase, diamonds to bcc phase.

can be suspected that intermixing of the two constituents occurs, even though the Al–Mo stability phase diagram does not report important mutual solubility at room temperature. Quantitative phase evaluation according to the Rietveld fit, reported in Fig. 3, shows a sudden increase of the initial bcc/fcc molar ratio 1:3 to saturation of ~1.45, immediately after 4 h. Of course, this evaluation is biased by having assumed only one metal species for each lattice.

The lattice parameter of the bcc phase does not show significant changes beyond the experimental uncertainty [Fig. 4(a)]. while that of fcc Al changes linearly as a function of MA time until 57 h of MA and then drops down [Fig. 4(b)]. Note that for the fcc case, the relative lattice parameter variation $\Delta a/a$ before and after prolonged times of milling amounts to 5.0×10^{-3}. The relative uncertainty of lattice parameters is correlated to peak broadening and, then, increases as a function of MA time. Varic *et al.*[22] have determined lattice parameters of the supersaturated solid solution (Al-rich side) retained by exceedingly rapid quenching. They measured a lattice parameter change $\Delta a/a$ of $\sim8\times10^{-4}$ for 1 at % of Mo solute, consequently, it can be supposed that at least 6% atomic of Mo is present in the Al matrix after 78 h of MA.

The trends of average crystallite size and mean squared lattice strain are reported in Fig. 5 as a function of milling time; it can be noted that a MA treatment is effective to reduce the average size domain to nanocrystalline range of dimension in a relative short time. The difference between

Downloaded 18 Nov 2008 to 192.167.65.40. Redistribution subject to AIP license or copyright; see http://jap.aip.org/jap/copyright.jsp

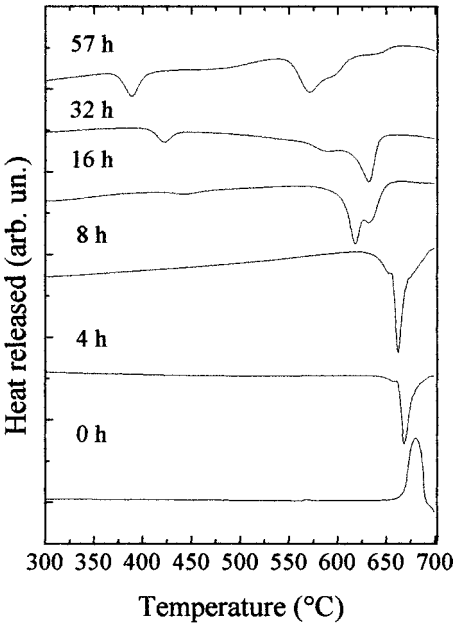

FIG. 6. DSC features of the specimens mechanically alloyed for the time indicated. The trace of the parental powder present an endothermic peak at 660 °C for the aluminum melting. Conversely, the feature of MA samples show complex exothermic peaks.

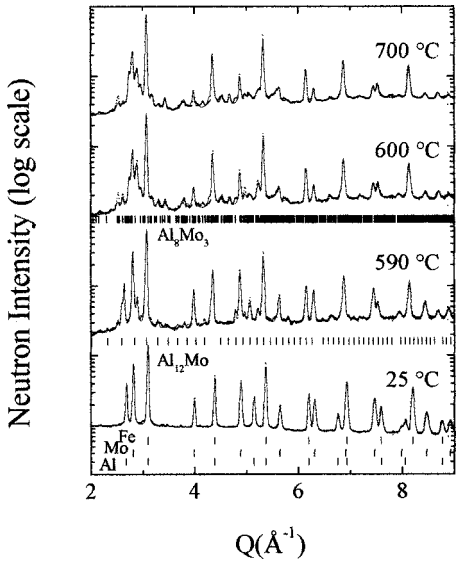

FIG. 7. Neutron diffraction patterns of specimen mechanically treated for 4 h and annealed at the temperatures quoted. The patterns show the presence of bcc iron peaks because of a misalignment of the support frame inside the furnace. Nevertheless, it was possible to envisage a phase transformation induced by the thermal treatment below 600 °C.

our size dimensions and those reported by Zdujic *et al.*[14,15] can be attributed to our methodology of pattern analysis as opposed to simple application of the Scherrer equation.

Partial or total disappearance of one phase during ball milling was reported in binary immiscible systems such as Cu–Fe, Cu–Co, Pd–Si, Ti–Si, Al–Ni.[23–27] In some cases, lattice parameter variations were not observed in the single phase remaining at the end of the process. On the other hand, our previous experience on the $Al_{75}Fe_{25}$ system (a binary mixture of fcc and bcc phases) has demonstrated that the mechanical treatment is able to make the fcc phase of Al completely dissolved in a bcc Al-rich solid solution with iron.[28] In that case, there was evidence of lattice parameter changes in the bcc dominant phase, accompanied by strong peak asymmetry. The disappearance of Si phase induced by MA in the Pd–Si system was attributed by Magini *et al.*[25] to the very fine crystallite size that affects drastically its x-ray absorption correction. If this would be true in the present case, then it should not be necessary to hypothesize occurrence of metastable solid solutions. However, nanocrystalline aluminum and iron milled separately and mixed together showed well visible diffraction peaks of fcc Al,[29] allowing to conclude that the absorption of x rays is governed by the amount of the substance and not by its submicron average crystallite size. Further, the DSC experiments on MA powders (Fig. 6) show exothermic peaks. This is opposed to the endothermic peak observed at 660 °C for the aluminum melting in the parental powders ($\Delta H = 0.388$ kJ/g).

We have been prompted by these considerations to devise an *in situ* annealing experiment for some as-milled powders and to verify possible occurrence of nonequilibrium solid solutions in contrast to simple highly fragmented mechanical mixtures of metallic compounds.

B. As-milled powders versus annealing

Neutron diffraction experiments with *in situ* annealing until 700 °C was performed just on four as-milled specimens, namely, those treated for 4, 32, 57, and 78 h. An appreciable background base line was present in the as-milled powders probably due to some inelastic scattering of hydrogen from ethanol, used as a lubricant agent. In all experiments, this background was eliminated from the closed vanadium can at ~400 °C. Unfortunately, a misalignment of the furnace made the neutron beam to irradiate the stainless steel support of the sample holder, which gave also strong iron peaks in the patterns, as it can be seen in the following figures. This is affecting to some degree the quality of numerical analysis of crystallographic phases.

Annealing of the specimen after MA for 4 h shows a phase reaction developing between ~590–600 °C (see Fig. 7). Initially the $Al_{12}Mo$ appears (space group I m 3,[30] $a=b=c=7.574$ Å), followed at 600 °C by the complete disappearance of fcc Al to give the Al_8Mo_3 phase (space group m C 22,[31] $a=9.27$ Å, $b=3.66$ Å, $c=10.17$ Å, $\beta=101.5$). After 600 °C, the $Al_{12}Mo$ phase disappear and hexagonal Al_5Mo phase[32] (space group $R-3c$ or $hp36$, $a=b=5.02$ Å, $c=26.83$ Å) is formed, likely at expenses of $Al_{12}Mo$ and unreacted bcc Mo. As expected, the lattice parameters values are larger than those reported in the literature, since the latter refer to room-temperature measurements.

According to the stability phase diagram of the Al–Mo system, revised recently by Schuster and Ipser,[32] $Al_{12}Mo$ should melt at 712 °C. This intermetallic, isostructural with $Al_{12}W$, is the first-order approximant for describing the relationship between icosahedral quasicrystals and their related crystalline structures.[30,33] This point has been discussed separately in another paper.[34]

Downloaded 18 Nov 2008 to 192.167.65.40. Redistribution subject to AIP license or copyright; see http://jap.aip.org/jap/copyright.jsp

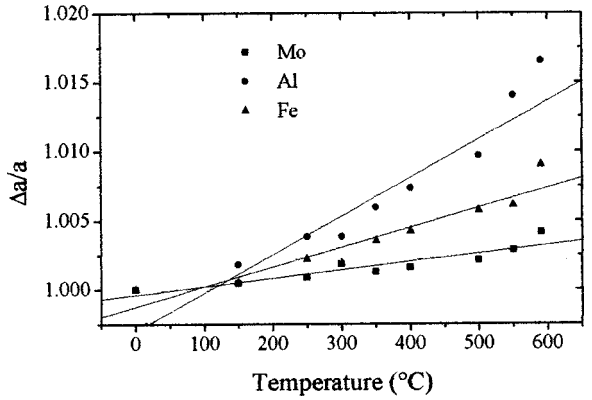

FIG. 8. Lattice parameter variation $\Delta a/a$ as a function of temperature for Al (circles), Mo (squares), and Fe (triangles) cubic phases, respectively.

Figure 8 shows the lattice parameter variation $\Delta a/a$ as a function of temperature for Al, Mo, and Fe cubic phases, respectively. The variations appear linear until 500 °C over an extended temperature range. In proximity of phase reaction the Mo curve shows a sudden increase.

A different reaction path was observed during annealing of the specimen treated for 32 h of MA (Fig. 9). At ~435 °C, the $Al_{12}Mo$ phase appears and increases its presence until ~490 °C, of course, at expenses of Al. At 500 °C, a sudden change in the structure occurs with the total disappearance of the bcc Mo-based phase, formation of Al_8Mo_3 and of a new Al_3Mo tetragonal phase not reported in the equilibrium phase diagram[25] [space group I 4/m m m or DO_{22}, $a=b=3.8075$ Å, $c=8.4369$ Å; Mo position in 2(a) (0 0 0), Al_1 in positions 2(b) (0 0 0.5); Al_2 in positions 4(d) (0 0.5 0.25)]. The occurrence of an analogous Al_5Mo_2Fe tetragonal phase reported by Pearson[35] [again space group I 4/m m m, where the Fe atom can be placed in 2(b) or 4(b)], has been excluded, since any significant presence of this element was detected by fluorescence analysis.

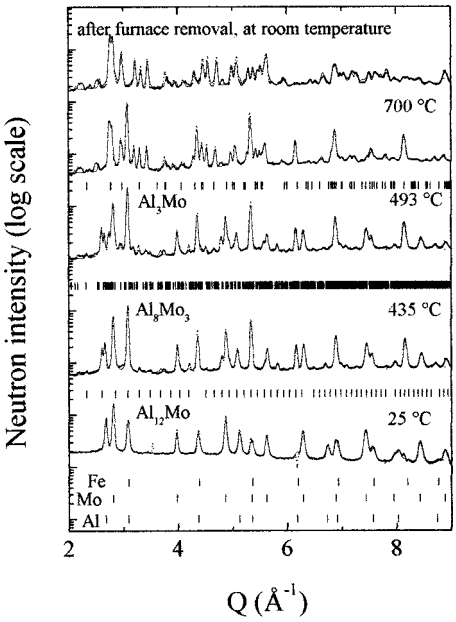

FIG. 9. Most representative neutron diffraction patterns of specimen mechanically treated for 32 h and annealed for the temperatures quoted. With respect to the specimen treated for 4 h, the occurrence of phase reactions is here anticipated and more complex. Moreover, at 500 °C, the sample is made of Al_8Mo_3 and a new Al_3Mo tetragonal phase.

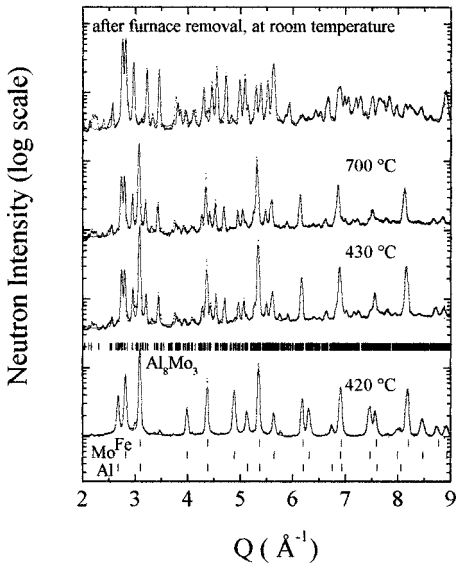

FIG. 10. Neutron diffraction patterns of specimen mechanically alloyed for 57 h and annealed up to 750 °C. There is a phase reaction at 430 °C when the fcc and bcc phases are transformed completely in the Al_8Mo_3 phase, which is reported stable up to 1550 °C in the phase diagram. At the top of the figure we have also reported the pattern obtained after cooling the cell and removal of the furnace. Very small extra peaks not accounted for by the Rietveld fit are likely to belong to a $FeVO_4$ phase of the vanadium can, since the same impurity peaks were not seen in the correspondent XRD pattern of the powder after its removal from the container.

Annealing of the specimen after 57 h of MA (Fig. 10) shows just one phase transition at ~430 °C and, again, iron peaks from the cell frame. Apart from iron, the remaining peaks are well described with the structure factor of the Al_8Mo_3 phase, indicating a total transformation of the reactants at moderately low temperature to afford a intermetallic compound melting congruently at 1550 °C. It was only after cooling of the specimen that the stainless steel sample holder was removed from the neutron beam. The pattern after annealing at 750 °C and cooled down to room temperature was accounted for satisfactorily by the fit using parameters of the Al_8Mo_3 phase with unit cell volume 0.6% smaller than that measured at high temperature.

Because of the removal of iron from the neutron beam, a better analysis of diffraction data was performed on *in situ* annealing of the specimen after 78 h of MA (Fig. 11). At 390 °C, the majority of the specimen is constituted by the Al_8Mo_3 and Al_3Mo phases, while the original fcc and bcc phases are still present but only in weak traces. These residual elemental phases disappear completely at 395 °C and subsequently the phase constitution does not appear to change until 700 °C.

In Fig. 12, we have plotted the temperature of appearance of the Al_8Mo_3 phase versus mechanical energy. The interesting linear behavior suggests that the formation of Al_8Mo_3 is assisted by the mixing induced by prolonged mechanical treatment. Since from Fig. 2 the intermixing of elements seems at a saturation level in the two phases already

Downloaded 18 Nov 2008 to 192.167.65.40. Redistribution subject to AIP license or copyright; see http://jap.aip.org/jap/copyright.jsp

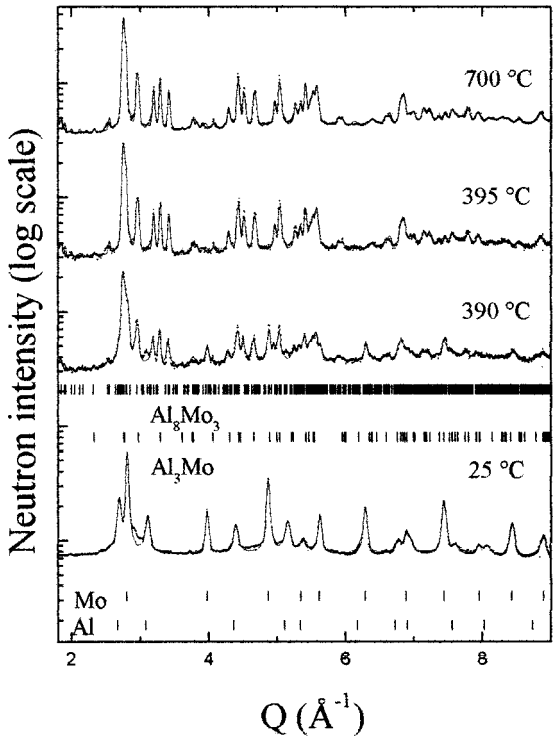

FIG. 11. Most important neutron diffraction patterns of specimen mechanically treated for 78 h. A transformation of the as-milled powder is observed at 390 °C, leading to monoclinic Al_8Mo_3 and tetragonal Al_3Mo phases.

after 4 h, we can advance the hypothesis that initially the formed solid solutions are heterogeneous in concentration (long-range fluctuations of composition) and later they become more homogeneous (with short-range fluctuations), as it can be argued also from the lattice parameter variation of Al reported in Fig. 3. Thus, the occurrence of different paths of reaction for phase formation can be explained by unpredictable local heterogeneity of the solid solution. A further problem arises if we want to answer why the Al_3Mo phase forms in specimens milled for 32 and 78 h but not in that treated for 57 h. This might be due to the fact that the latter specimen was heated with a ramp velocity higher than the

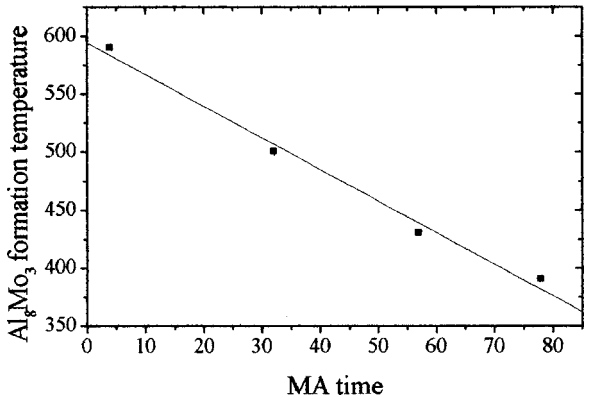

FIG. 12. Temperature of appearance of the Al_8Mo_3 phase as a function of mechanical treatment time. The observed linear behavior as a function of treatment time suggests that the solid solutions are becoming more and more homogeneous in concentration, i.e., very similar in their short-range order properties.

formers. In any case, the above data support the hypothesis that the as-milled powders are composed of extended solid solutions, in spite of their lattice parameters have not changed considerably during MA.

Colgan, Nastasi, and Mayer[36] have studied the Al–Ni thin films fabricated by sequential evaporation and coevaporation and further annealed under vacuum. They suggested that the kinetics rather than the thermodynamics is responsible for the phase growth, because of the high mobility of Al atoms. Forrester and Schaeffer[37] studying the mechanism of self-sustaining high-temperature combustion syntheses concluded that diffusion is the rate controlling step and mechanically induced solid state reactions can occur when short-circuit diffusive paths are generated. Of course, the diffusive short-circuit paths strongly depend on the strain accumulation rate in the main lattice.

It is interesting to note that Zdujic *et al.*[14] observed, for a composition close to that of our specimens, the occurrence of Al_8Mo_3 phase at higher temperature (1000 °C), which can be also ascribed to different ball milling apparatuses. However, a complementary analysis on the same powders after DSC[38] seems to suggest that the external pressure applied to the samples may change considerably the kinetics of intermetallic formation, due to different competing growth phenomena.

IV. CONCLUSIONS

High-energy ball milling of $Al_{75}Mo_{25}$ elemental powders produces fcc Al(Mo) and bcc Mo(Al) nanocrystalline solid solutions, as determined from the Rietveld analysis of diffraction patterns and neutron small angle data. Exothermic events recorded in the DSC traces up to 700 °C suggest that these solutions are metastable. For the specimens mechanically treated for 32 and 78 h, annealing experiments under high vacuum at a neutron diffraction instrument revealed a new Al_3Mo tetragonal phase, isostructural with Al_3Ti or with Al_5Mo_2Fe, coexisting in some cases with the Al_8Mo_3 phase. The tetragonal phase was not found in the specimen treated for 57 h. This effect can be attributed to different heating rate and work is in progress to investigate the phase formation as a function of increasing temperature rate.

In addition to this, the cubic $Al_{12}Mo$ phase was observed, which is classified as first-order crystalline approximant of a quasicrystalline structure. In fact, the Mo atoms are arranged according to a bcc lattice and surrounded icosahedrally by 12 Al atoms. In turn, these icosahedra are related one to each other by octahedra.

The temperature of the appearance of Al_8Mo_3 in annealed alloys decreases almost linearly as a function of the mechanical treatment time.

Further crystallographic work with the Rietveld method on alloys annealed at normal pressure in a DSC instrument has revealed a different phase selection of end-products.[38] There might be further merit to investigate the opportunity of creating new metastable phases as a function of external pressure applied during annealing of powders.

Downloaded 18 Nov 2008 to 192.167.65.40. Redistribution subject to AIP license or copyright; see http://jap.aip.org/jap/copyright.jsp

ACKNOWLEDGMENTS

This research is part of a project supported by MURST (former funding 40%) and CNR of Italy. The authors acknowledge the Institute Laue-Langevin, Grenoble, France, in providing the neutron research facilities (experiment No. 5-26-024). The small angle neutron measurements were supported with the help of the CLRC (RB 8745) and by European Community (TMR Program for Large Scale Facilities and TMR project No. ERB FMRX-CT9801621). The authors acknowledge also the staff of D20 diffractometer at ILL, Grenoble and Dr. P. Radaelli, the staff of LOQ, RAL, Chilton (UK), and Dr. R. K. Heenan. Thanks are due to Dr. L. Lutterotti (Università di Trento, Italy) for making available a copy of RIETQUAN code running on a personal computer.

[1] C. C. Koch, Nanostruct. Mater. **9**, 13 (1997).
[2] E. Gaffet, Mater. Trans., JIM **36**, 198 (1995).
[3] R. W. Siegel and G. E. Fougere, in *Nanophase Materials*, edited by G. C. Hadjipanais and R. Siegel (Kluwer, Dordrecht, 1994). p. 233.
[4] R. L. Valiev, Nanostruct. Mater. **6**, 73 (1995).
[5] C. Suryanarayana, Int. Mater. Rev. **40**, 41 (1995).
[6] M. A. Morris and D. G. Morris, Mater. Sci. Forum **88–90**, 271 (1992).
[7] T. Zàk, O. Schneiweiss, Z. Cochnar, and A. Buchal, Mater. Sci. Eng., A **141**, 73 (1991).
[8] D. Oleszak and P. H. Shingu, Mater. Sci. Eng., A **181/182**, 1217 (1994).
[9] E. Bonetti, G. Scipione, G. Valdré, G. Cocco, R. Frattini, and P. P. Macrì, J. Appl. Phys. **74**, 2053 (1993).
[10] E. Bonetti, G. Scipione, R. Frattini, S. Enzo, and L. Schiffini, J. Appl. Phys. **79**, 7537 (1996).
[11] S. Enzo, R. Frattini, R. Gupta, P. P. Macrì, G. Principi, L. Schiffini, and G. Scipione, Acta Mater. **44**, 3105 (1996).
[12] C. N. J. Wagner, in *Local Atomic Arrangements Studied by X-ray Diffraction*, edited by J. B. Cohen and J. E. Hilliard (Plenum, New York, 1996), p. 219.
[13] M. Zdujic, F. Kobayashi, and P. H. Shingu, Z. Metalkd. **81**, 391 (1990).
[14] M. Zdujic, F. Kobayashi, and P. H. Shingu, J. Mater. Sci. **26**, 5502 (1991).
[15] M. Zdujic, D. Poleti, Lj. Karanovic, K. F. Kobayashi, and P. H. Shingu, Mater. Sci. Eng., A **185**, 77 (1994).
[16] *The Rietveld Method*, edited by R. A. Young (International Union of Crystallography, Oxford University Press, Oxford, 1993).
[17] J. Rodriguez-Carvajal, Physica B **192**, 55 (1993).
[18] L. Lutterotti and S. Gialanella, Acta Mater. **46**, 101 (1998).
[19] P. Rose, D. E. Banda, N. Cowlam, and S. Enzo, Mater. Sci. Forum **179–181**, 787 (1995).
[20] P. P. Macrì, D. E. Banda, P. Rose, S. Enzo, and N. Cowlam, Mater. Sci. Forum **179–181**, 793 (1995).
[21] S. Enzo, R. Frattini, P. Canton, G. Mulas, and P. Radaelli, Nanostruct. Mater. **12**, 547 (1999).
[22] N. I. Varic, L. M. Burov, K. Ja. Kolesnicenko, and A. P. Maksimenko, Phys. Met. Metallogr. **15**, 111 (1963).
[23] S. Enzo, G. Mulas, R. Frattini, R. J. Cooper, N. Cowlam, and G. Principi, Philos. Mag. **76**, 471 (1997).
[24] M. Baricco, N. Cowlam, L. Schiffini, P. P. Macrì, R. Frattini, and S. Enzo, Philos. Mag. B **68**, 957 (1993).
[25] M. Magini, N. Burgio, S. Martelli, F. Padella, E. Paradiso, and G. Ennas, J. Mater. Sci. **26**, 3969 (1991).
[26] N. Malhouroux-Gaffet and E. Gaffet, J. Alloys Compd. **198**, 143 (1993).
[27] M. A. Atzmon, Phys. Rev. Lett. **22**, 487 (1990).
[28] S. Enzo, R. Frattini, G. Mulas, and F. Delogu, Mater. Sci. Forum **269–272**, 391 (1998).
[29] E. Bonetti, G. Scipione, G. Valdré, S. Enzo, R. Frattini, and P. P. Macrì, J. Mater. Sci. **30**, 2220 (1995).
[30] J. Adam and J. B. Rich, Acta Crystallogr. **7**, 813 (1954).
[31] J. B. Forsyth and G. Gran, Acta Crystallogr. **15**, 100 (1962).
[32] J. C. Schuster and H. Ipser, Metall. Trans. **22A**, 1729 (1991).
[33] A. P. Tsai, MRS Bull. **22**, 43 (1997).
[34] S. Enzo, G. Mulas, F. Delogu, and R. Frattini, J. Metastable Nanocryst. Mater. **2–6**, 417 (1999).
[35] *Handbook of Lattice Spacings and Structures of Metals and Alloys*, edited by W. B. Pearson (Pergamon, Oxford, 1964).
[36] E. G. Colgan, M. Nastasi, and J. W. Mayer, J. Appl. Phys. **58**, 4125 (1985).
[37] J. S. Forrester and G. B. Schaeffer, Metall. Trans. **26A**, 725 (1995).
[38] M. Monagheddu, F. Delogu, L. Schiffini, R. Frattini, and S. Enzo, Nanostruct. Mater. (in press).

Downloaded 18 Nov 2008 to 192.167.65.40. Redistribution subject to AIP license or copyright; see http://jap.aip.org/jap/copyright.jsp